Proceedings of the EuroGNC 2013, 2nd CEAS Specialist Conference on
Guidance, Navigation & Control, Delft University of Technology, Delft,
The Netherlands, April 10-12, 2013

The Total Energy Control Concept for a Motor Glider

Maxim Lamp, Robert Luckner

Abstract In this article the Total Energy Control System (TECS) that was introduced by Lambregts to control the vertical flight path and the velocity of an aircraft by using the total energy and the energy distribution between the flight path and the acceleration, will be taken up, modified, extended and tested on a motor glider. The TECS concept has been extended by using the airbrakes as additional control elements to manipulate the total energy. For motor gliders and utility aircraft with a high glide ratio this increases the sink performance and the range of possible missions, like steep approaches. Further modifications are done to improve the height accuracy during normal operation and during flare manoeuvre and to improve the control response reaching its saturations. A height protection is introduced to make a safe flight near to the ground possible. The usage and generation of required sensor signals from existing sensor data is introduced. Examples of flight test results are given.

Maxim Lamp, research scientist,
Berlin Institute of Technology, Department of Flight Mechanics, Flight Control and Aeroelasticity,
e-mail: Maxim.Lamp@ilr.tu-berlin.de

Robert Luckner, Professor
Berlin Institute of Technology, Department of Flight Mechanics, Flight Control and Aeroelasticity,
e-mail: Robert.Luckner@ilr.tu-berlin.de

Nomenclature and Abbreviations

C_D	$[-]$	drag coefficient
C_L	$[-]$	lift coefficient
C_m	$[-]$	moment coefficient
E_{dist}	$[Nm]$	energy distribution
E_{kin}	$[Nm]$	kinetic energy
E_{pot}	$[Nm]$	potential energy
E_{spec}	$[Nm]$	specific energy
E_{tot}	$[Nm]$	total energy
F_D	$[N]$	drag force
F_G	$[N]$	weight force
F_T	$[N]$	thrust force
H	$[m]$	height
K	$[...]$	gain
P	$[Nm/s]$	power
V	$[m/s]$	velocity
g	$[m/s^2]$	constant of gravitation
m	$[kg]$	mass
n	$[g]$	acceleration
Θ	$[rad]$	pitch angle
Φ	$[rad]$	bank angle
γ	$[rad]$	flight path angle

Indizes

0	intial value
A	aerodynamic
K	flight path
W	Wind
cas	calibrated airspeed
cmd	command
f	body fixed coordinate frame
max	maximum
min	minimum
res	resulting
tas	true airspeed

Abbreviations

AD	Air Data System
AFCP	Automatic Flight Control Panel
AFCS	Automatic Flight Control System
AW	Anti Wind-Up
FCL	Flight Control Laws
GNSS	Global Navigation Satellite System
GPS	Global Positioning System
MSU	Magnet Sensor Unit
TECS	Total Energy Control System

1 Introduction

The aim of the research project LAPAZ[1] is to develop and to demonstrate an Automatic Flight Control System (AFCS) [5]. The AFCS is developed for a single engine, long-endurance motor glider, the STEMME S15 of the German aircraft manufacturer STEMME. The Flight Control Laws (FCL) of the AFCS provide a high-precision flight path control, automatic navigation control along 3D trajectories and automatic landing as well as automatic takeoff functions [11]. It can be used in piloted and unmanned operations (optionally piloted).

Since the aircraft is a motor glider with a high glide ratio, it can be used for long endurance missions at high altitudes. To use those attributes, it is of advantage that the FCL consider the total energy of the flying system as Lambregts has shown, when he introduced the Total Energy Control System (TECS). TECS uses thrust and elevator to control the total energy and the energy distribution [6] – [10]. This concepts is characterized by a simple structure that relates to laws of physics and can be easily adopted to different aircraft types.

[1] "Luftarbeitsplattform für die Allgemeine Zivilluftfahrt", aerial work platform for general aviation

In [6] the thrust, receptively the engine is used as the only control element to modify the total energy. If the engine is in idle position, a further reduction of the total energy is not possible. That means the largest achievable sink rate in stationary flight is a function of the geometric configuration and aerodynamic characteristic of the aircraft. Especially during descents with simultaneous deceleration, e.g. landing approaches, the sink performance can limit the mission scope. Using a glider or a motor glider with high glide ratio, the usage of airbrakes is an adequate option to control the total energy by varying the drag force.

In the FCL of the LAPAZ project, the existing TECS concept has been taken up, modified and extended. Figure 1 depicts the TECS core system from [6]. It can be divided into a total energy and an energy distribution control path. Section

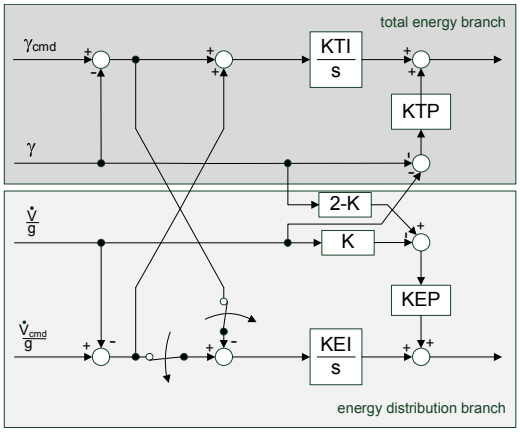

Fig. 1 Basic Total Energy Control System from [6]

2 discusses the total energy and thrust branch, Sect. 4 the energy distribution and elevator branch.

One significant change is the usage of the airbrakes as an additional control element. Other changes address the improvement of the height accuracy, the possibility to use TECS during flare manoeuvres and of the behaviour of the control elements reaching their saturation.

2 Using the Total Energy Control Concept with Airbrakes

This section describes the control concept that Lambregts introduced in [6] – [10]. After a brief repetition of the theoretical aspects, the control concept will be expanded.

If the rotational energy is neglected, the total energy E_{tot} is the sum of kinetic energy E_{kin} and potential energy E_{pot} and can be expressed as

$$E_{tot} = E_{pot} + E_{kin} = \frac{m}{2} \cdot V_K^2 + m \cdot g \cdot H \tag{1}$$

with aircraft mass m, height H, flight path velocity V_K and gravitational constant g. Under the assumption of constant mass, the excess power is given by

$$\frac{\dot{E}_{tot}}{F_G} = \frac{V_K \cdot \dot{V}_K}{g} + \dot{H} \quad . \tag{2}$$

A division by the flight path velocity yields to the specific energy rate $\dot{E}_{spec}$, where F_G is the weight force and the dot indicates the time derivative leads to

$$\dot{E}_{spec} = \frac{\dot{E}_{tot}}{F_G \cdot V_K} = \frac{\dot{V}_K}{g} + \frac{\dot{H}}{V_K} \tag{3}$$

$$\dot{E}_{spec} = \frac{\dot{V}_K}{g} + sin(\gamma) \quad . \tag{4}$$

The specific energy rate represents a measure of the system's energy gain or loss. Simplifying the aircraft as a point mass in an inertial system without wind, the second axiom of motion along the flight path leads to

$$m \cdot \dot{V}_K = F_T - F_D - sin(\gamma) \cdot F_G \quad , \tag{5}$$

where F_T is the thrust force, F_D is the drag force and F_G is the weight.

Assuming small flight path angles $(sin(\gamma) \approx \gamma)$ and by comparison of eq. (4) and eq. (5) the specific energy rate can be expressed by

$$\dot{E}_{spec} = \frac{\dot{V}}{g} + \gamma = \frac{F_T - F_D}{F_G} \quad . \tag{6}$$

This obvious shows, that the thrust force and the drag force can be used to influence $\dot{E}_{spec}$ and thus the total energy of the system. In stationary flight the total energy is balanced, thrust force and drag force must be equal $F_{D_0} = F_{T_0}$. In this case the specific energy rate is zero. A change in total energy can be achieved by changing the thrust and drag forces individually or simultaneously

$$F_G \cdot \Delta\dot{E}_{spec} = F_G \cdot \left(\frac{\Delta\dot{V}_K}{g} + \Delta\gamma \right) \quad . = \Delta F_T - \Delta F_D \tag{7}$$

At this stage the assumption of no wind $V_K = V_A$ was made. That may imply, that TECS uses only kinetic and potential energy in a pure physical sense. However, flight control has to fulfil multiple requirements, depending on flight phase and mission objectives. In many flight phases the objectives regard the airspeed, close to the ground, flight path velocity becomes important. The velocity equation $V_K = V_A + V_W$, that relates flight path velocity V_K, airspeed V_A and wind velocity V_W, indicates that it is not possible to control V_K and V_A at the same time, when the wind velocity changes. Additionally, it is not simple to measure flight path velocity

and flight path angle with high bandwidth and accuracy over the full flight envelope. Depending on the available sensors, compromises have to be found. Instead of using V_K, $\dot{V}_K$ and γ the measured and estimated signals V, $\hat{\dot{V}}$ and $\hat{\gamma}$ that are explained in Sect. 5 will be used in the FCL.

In the concept of the Total Energy Control System [6]–[10], the only control element to modify the total energy is the thrust force, respectively the engine. To generate a thrust command, an integral controller (I-controller) with a proportional feedback is used. Here, the total energy control concept will be expanded by using the airbrakes as an additional control element. There are two possibilities to integrate the airbrakes as a control element into the existing controller concept.

The first possibility is to use the existing linear controller to compute an incremental force command ΔF, which can be divided into incremental thrust force and drag force commands, see Fig. 2. Those commands can then be converted into appropriate engine or airbrake commands. In the simplest case, thrust and drag forces can be commanded by using a function that computes airbrake commands if the engine is at idle. The advantage of this concept is the simple structure of the control law, because only one controller has to be designed. However, the dynamic behaviour and the effectiveness of the engine and the airbrakes are different, which will be shown in Sect. 3. With the design of only one linear controller these differences cannot be directly considered, which is a significant disadvantage.

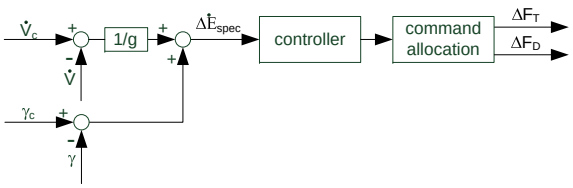

Fig. 2 Control of specific energy rate by one controller and subsequent separation into incremental thrust and drag force commands.

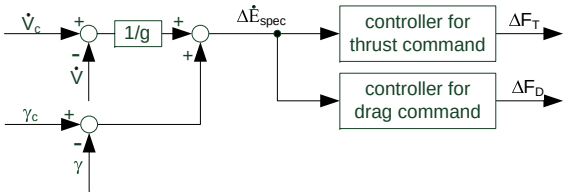

Fig. 3 Control of specific energy rate by using individual controllers for incremental thrust and drag force commands.

The second possibility is to use two separate linear controllers, one to compute the required incremental thrust force ΔF_T and one to compute the required incremental drag force ΔF_D, as can be seen in Fig. 3. These two controllers can be designed independently and can have different structures, which allows taking the dif-

ferences in dynamic behaviour and effectiveness of the two control elements into account. Simultaneous use of both control elements is also possible. This can be an advantage for example during landing approaches in turbulent atmospheric conditions and if large engine activity has to be avoided. During the approach the engine can run approximately constant, while the airbrakes can be used to correct gusts or wind shear disturbances. The concept also has a beneficial effect in case of a missed approach (Go Around) manoeuvre. By retracting the airbrakes in this case, the drag is reduced rapidly while the total lift coefficient increases.

As with the first concept, there are also disadvantages. Within the control ranges of the control elements there are unlimited possible combinations of thrust and drag commands, including undesirable combinations. For example, cruise flight with partially extended airbrakes and simultaneous increased thrust setting could be conceivable, which will result in excessive fuel consumptions. This problem can be solved either by using different dynamics for the respective controllers or by using logical switching.

For the FCL of the LAPAZ project, a control structure based on the second concept is used. The usage of the airbrakes is optional and can be switched on and off. Figure 4 shows the structure of the total energy controller. The incremental thrust command ΔF_T results from the deviation of the specific energy rate and is controlled by using an I-controller, combined with a proportional feedback of the potential flight path angle $(\hat{\dot{V}}/g + \hat{\gamma})$, similar to [6]. A difference to the scheme in [6] is the feedback of the signal $(\hat{\dot{V}}/g + \hat{\gamma})$, which is subtracted behind the integrator in the original control scheme. In the control concept here, it is subtracted before the integrator. In order to do so, it must be differentiated first. The final outcome of this signal by differentiation and subsequent integration remains the same: $\frac{\hat{\dot{V}}}{g} + \hat{\gamma} = \int \frac{\hat{\dot{V}}/g+\hat{\gamma}}{dt} dt$. Because the feedback signal is subtracted before the integrator it is cancelled when the anti wind-up control is active. As a result the feedback will not lead to unwanted thrust commands when thrust is saturated, especially in turbulent atmospheric conditions where disturbances in $\hat{\gamma}$ and $\hat{\dot{V}}$ will directly influence the thrust command.

Figure 5 shows a simulation study to demonstrate the reaction of the throttle by adding the feedback of the potential flight path angle before and behind the integrator. The simulation starts at a descent with a vertical speed of approximately $\dot{H} = -1.8\,m/s$ and an airspeed of $V_{cas} = 130\,km/h$. The throttle is in idle (8%). At time t=96 s, turbulence is activated with a standard deviation of about $0.5\,m/s$. Until time t=120 s the damping feedback was added before the integrator, afterwards it was added behind the integrator. As can be seen, the throttle command is much smoother when the feedback is added in front of the integrator. The bottom plot of Fig. 5 depicts the throttle command $thro_{cmd}$ and the true throttle position at engine. It shall be noted, that the simulation model includes friction, hysteresis and elasticity of the throttle actuator and the control linkage between the actuator and the throttle at the engine.

To compute the required incremental drag force and subsequent airbrakes command, an I-controller is used. Its output can be regarded as an airbrakes trim. The

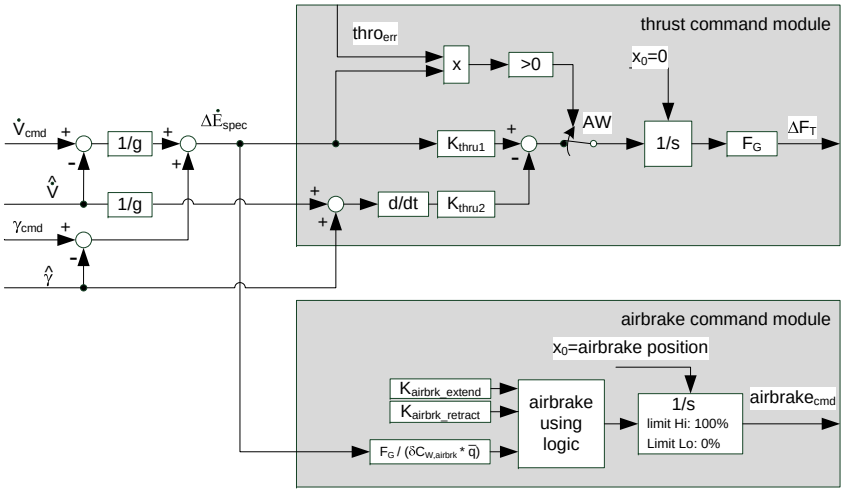

Fig. 4 Control scheme for total energy control with thrust and airbrakes commands.

dynamics of the airbrakes command controller are different for the case of airbrakes extension and retraction. The gain for retraction is higher than the gain for extension. In case of retraction this prevents from using the airbrakes and the throttle together at the same time. Beside of this, the safety increases in case of retraction. The behaviour in case of extension can be adjusted to fit with the throttle behaviour, so that, after reaching idle, a commanded total energy reduction can command the airbrakes in a way that the behaviour is the same as with reduction of throttle. A logic prohibits that the airbrakes are further extended during turn.

The motor glider STEMME S15 is equipped with a single piston engine with an adjustable propeller. The FCL generate throttle and propeller revolution commands to drive the engine at its best performance. Figure 6 depicts schematically the structure of the engine command module. The incremental thrust command ΔF_T together with the airspeed and the propeller efficiency are converted to an incremental power command ΔP. This is send to an integrator with a very low time constant, which output can be regarded as a trim of power. The throttle command is computed from the sum of the trimmed power and the incremental power command. The absolute value is limited. An engine protection function prevents the engine to exceed the maximum allowable rotation speed by limiting the throttle command ratio. Unlike in [6] there is no knowledge about the current net thrust nor the engine pressure ratio (EPR) and no performance prediction model of the engine is used to determine the maximum and minimum power. So these informations cannot be used to prevent a wind-up of the integrator in the total energy controller. The anti wind-up is achieved here by using the difference between the throttle command and the throttle command limit to feed an anti wind-up switching logic (AW) in the engine command module and in the thrust command module, see Fig. (4) and Fig. (6).

3 Analysis of Throttle and Airbrakes Responses

A simulation analysis, using the non-linear aircraft model of the motor glider STEMME S15 and the AFCS model was conducted to analyse the differences in reaction of total energy due to step changes in throttle setting and airbrake deflection. The simulation includes the dynamic behaviour of the engine and the airbrakes. The initial trimmed condition was a steady descent with a vertical speed of $\dot{H} = -1.5\,m/s$ and an airspeed of $V = 130\,km/h$. The throttle and the airbrakes control loops were opened and throttle and airbrakes were directly stimulated in the aircraft simulation model. The dynamic behaviour of the engine and airbrakes are included. While one control element was stimulated at a time, the respective other

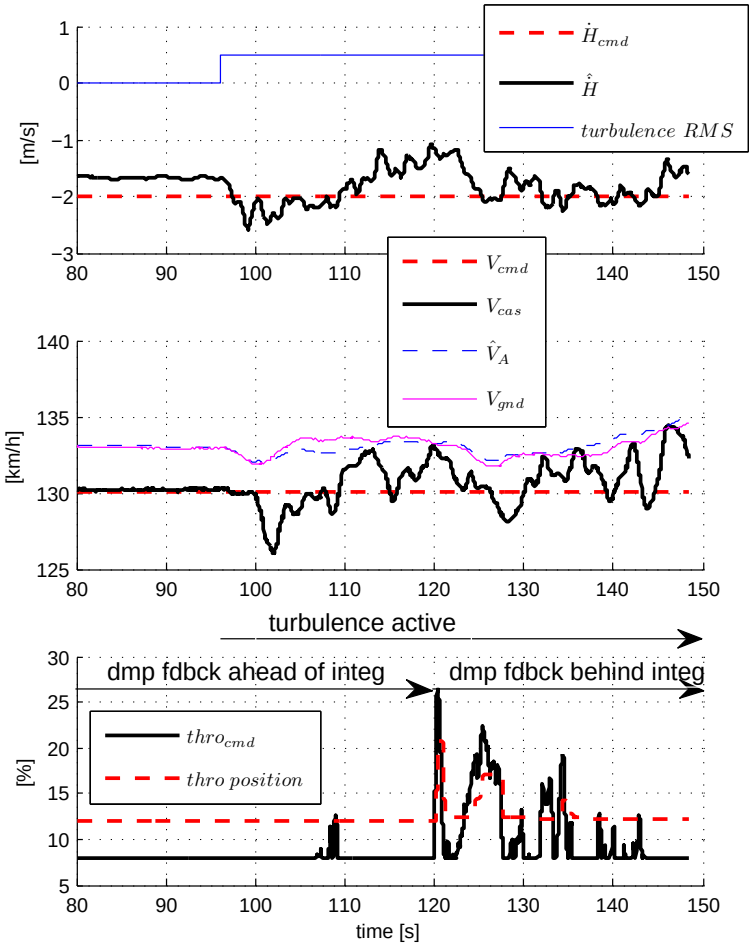

Fig. 5 Simulation results, proportional feedback before and behind the integrator.

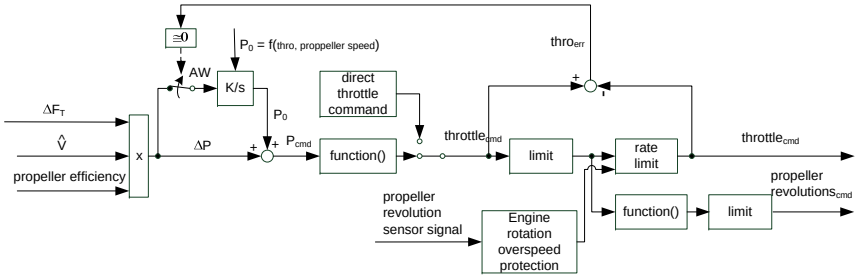

Fig. 6 Scheme of the engine command module.

control element was held at its position. The elevator command loop stayed closed. Thus the FCL commanded the elevator to compensate the flight path deviation (*flight path priority*, as described in Sect. 4).

Figure 7 shows the responses of the specific total energy rate $\dot{E}_{spec}$ (Fig 7a and 7e), of the deviation of specific total energy rate $\Delta\dot{E}_{spec}$ (Fig 7b and 7f), of the flight path deviation $\Delta\gamma$ (Fig 7c and 7g) and of the deviation of acceleration along to flight path $\Delta\dot{V}/g$ (Fig 7d and 7h) due to increase of throttle command $thro_{cmd}$ and decrease of the airbrake command $airbrk_{cmd}$ and vice versa. During the simulation the total energy was reduced by decreasing the throttle command from the 50% to 30% or by extending the airbrakes from 50% to 70%, see Fig. 7 a-d. Comparing the deviations of the total energy rates, it can be seen that the airbrakes are somewhat more effective in the initial reaction than the throttle. Both control elements mainly produce changes in the flight path acceleration, see Fig. 7 c. The deviations in the flight path angle are small, as it is controlled by the elevator.

Simulations with appropriate control deflections to increase total energy were also performed, see Fig. 7 e-h. With respect to total energy, both control elements have approximately the same effect. While a step change in throttle mainly leads to a deviation in the flight path acceleration, a step in airbrake deflection leads to deviations in the flight path acceleration and the flight path angle. The deviation in the flight path angle is later reduced by elevator deflections commanded by the FCL. The error in the flight path acceleration remains.

In addition to the change in drag, the airbrakes also generate a change in the total lift coefficient of the aircraft and in the pitching moment, see Fig. 8. So it is possible to manipulate not only the drag, which means the path acceleration, but also the lift, which means the flight path. Thus the airbrakes are well suited for simultaneous velocity and flight path changes, e.g. for simultaneous deceleration and descent during initiation of landing approach.

Figure 8 shows that the change of the lift coefficient due to airbrake extension is non-linear. The gradient goes to zero beyond the 50% position. That is why the reaction in the deviation of the flight path is so small during the experiments where the airbrakes were extended from 50% to 70%. It must be taken into account, that the airflow around the wing induced by the propeller is not modelled in the simulation model. This will also impact the total lift of the aircraft.

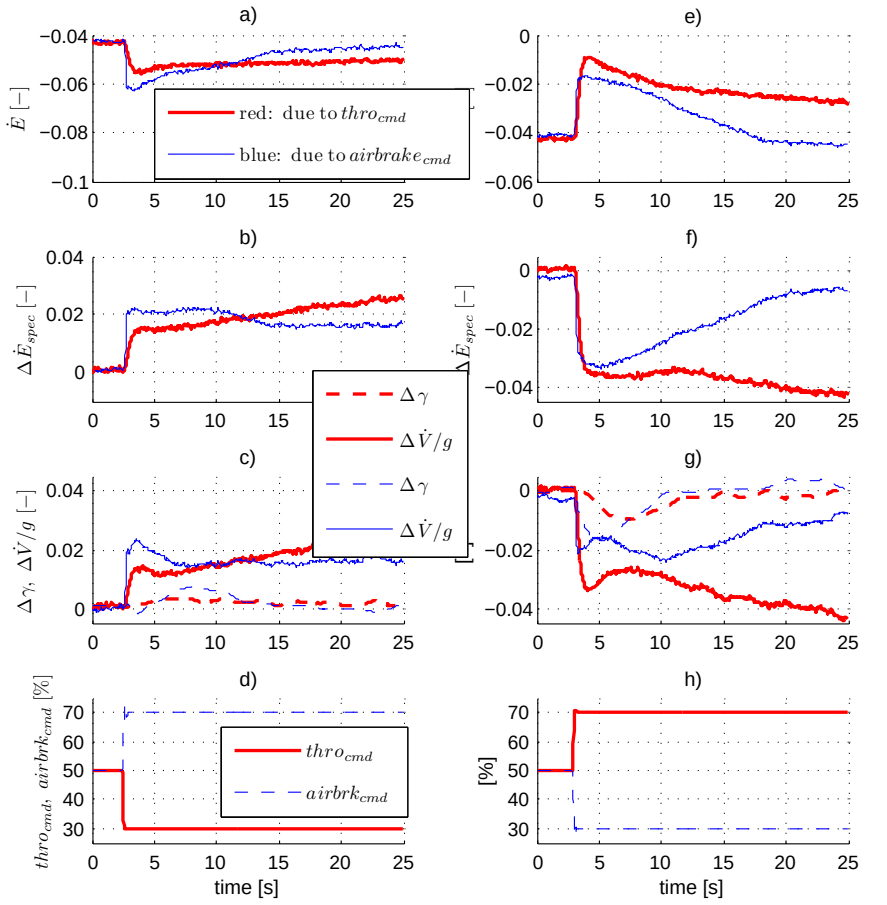

Fig. 7 Step responses of throttle and airbrake commands, regarding to specific energy rate.

4 Modification of the Energy Distribution Concept

The redistribution of the total energy between the kinetic and potential energy can be achieved by using the elevator, as described in [6] or by pitch attitude as in [12]. This latter method is adopted here. If there is no change in total energy, that means $\Delta\dot{E}_{spec} = \frac{\Delta\dot{V}}{g} + \Delta\gamma = 0$, an increase in potential energy results in a reduction of kinetic energy and vice versa

$$-\frac{\Delta\dot{V}}{g} = \Delta\gamma \quad . \tag{8}$$

According to [6] the energy distribution error $\Delta\dot{E}_{dist}$ is defined by

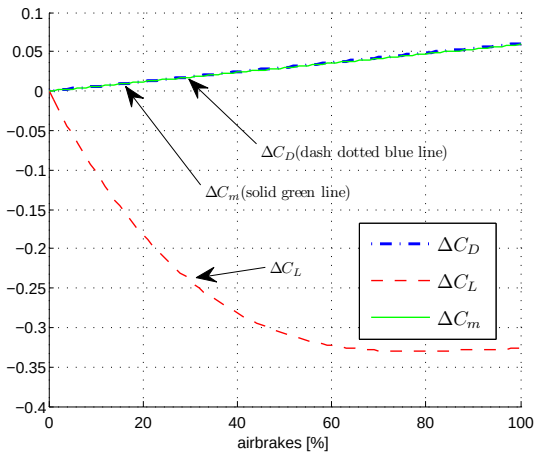

Fig. 8 Changes in lift, drag and pitching moment coefficients due to airbrake deflection.

$$\Delta \dot{E}_{dist} = -\frac{\Delta \dot{V}}{g} + \Delta \gamma \quad . \tag{9}$$

Reducing this energy distribution error to zero means that the total energy rate is divided equally in potential and kinetic energy. This concept of equal distribution into potential and kinetic energy is used in [6] and other studies, if the engine is not saturated. If the engine is saturated, concepts are proposed which prioritize the energy distribution in favour of the potential or kinetic energy. This is called *flight path priority* and *speed priority*. In those cases the elevator controls the velocity respectively the flight path angle. By using speed priority, a speed protection can be achieved [6]. The commanded must not be lower than the allowed minimum speed or greater than the maximum speed.

By designing the total energy controller and the energy distribution controller with the same dynamic behaviour, a decoupling of the longitudinal and the vertical control axes of the aircraft can be achieved [6]. The slow dynamic behaviour of the engine limits the bandwidth for achieving pure flight path and speed control decoupling.

Since the change of the total energy is a function of the dynamic behaviour and the effectiveness of the engine or the airbrakes, it cannot be assured that the deviation in total energy rate, for example due to a change of the velocity command or due to a wind disturbance, can be reduced rapidly. In that case the concept of equal distribution of total energy into potential and kinetic energy may lead to a deviation in both, in flight path angle and in velocity.

In the LAPAZ project, high-precision flight path following is required. To minimize the path deviation, deviations in airspeed are allowed, as long as they are not violating the speed envelope. The flight path priority is used as the standard mode to distribute the energy. In the LAPAZ demonstrator the pilot has the possibility to limit the vertical speed manually and by this to control the direction of the en-

ergy distribution. This can be done via an Automatic Flight Control Panel (AFCP), designed especially for the LAPAZ demonstrator.

To detect a violation of the permitted speed envelope while using flight path priority, a resulting acceleration command $\dot{V}_{cmd,res}$ is computed based on the deviation in flight path angle $\Delta\gamma$ and the current path acceleration $\hat{\dot{V}}$

$$-\frac{\Delta\dot{V}}{g} = \Delta\gamma \qquad \text{with} \quad \Delta\dot{V} = \dot{V}_{cmd,res} - \dot{V} \tag{10}$$

$$\dot{V}_{cmd,res} = -\Delta\gamma \cdot g + \dot{V} \quad . \tag{11}$$

A comparison of the resulting acceleration command with the acceleration commands corresponding to the minimum and the maximum speeds ($\dot{V}_{min}$ and $\dot{V}_{max}$) conduct the priority switching logic to switch to speed priority. By using the minimum and maximum acceleration commands, which are calculated by current mass, altitude and flap setting, a speed priority is realized.

Lambregts introduces in [6] a similar value $\dot{V}_{max} = \dot{V} + \gamma \cdot g$ which in case of engine saturation limits the acceleration, so that a maximum level ($\gamma = 0$) acceleration/deceleration can be obtained. Unlike here the value $\dot{V}_{cmd,res}$ is not calculated by using γ but by using the flight path deviation $\Delta\gamma$. The resulting acceleration command is not used for limiting the acceleration, instead it is used to trigger the priority switch, as described before.

In an earlier version of the FCL, the only possibility to regulate the energy distribution during descent while the flight path priority was active, was to command the vertical speed. Flight tests in the course of the LAPAZ project have shown, that while using flight path priority during descent, this can confuse the pilot. For example, the pilot tried to reduce the increasing velocity during descent with high sink rate and throttle at idle by reducing the commanded velocity instead by reducing the sink rate, not regarding, that the velocity error is not controlled during flight path priority. This finding resulted in the requirement to use speed priority during descent if the control elements to control the total energy are saturated.

In [6] a linear I-controller with a proportional feedback was introduced to compensate the energy distribution error. This controller concept is used in a modified form here. Figure 9 shows the scheme of the energy distribution controller. The module *energy distribution control priority logic* contains the priority switching logic. Compared with the structure in [6] the proportional feedback does not contain the path acceleration $\dot{V}$. This design choice reduces unwanted pitch commands in turbulent atmospheric conditions.that would be induced by $\dot{V}$ feedback.

Furthermore, after differentiating, the feedback signal $\hat{\gamma}$ is subtracted before the integrator instead of behind, as in the *total energy control module*, see Fig. 4.

The integrator is initialized with the current pitch attitude angle. Together with the commanded incremental changes the integrator computes an absolute pitch attitude command for the inner loop pitch controller. Adding an attitude trim variable Θ_0, as in [12] is not necessary, since the integrator output is the total pitch attitude command and not an incremental attitude command.

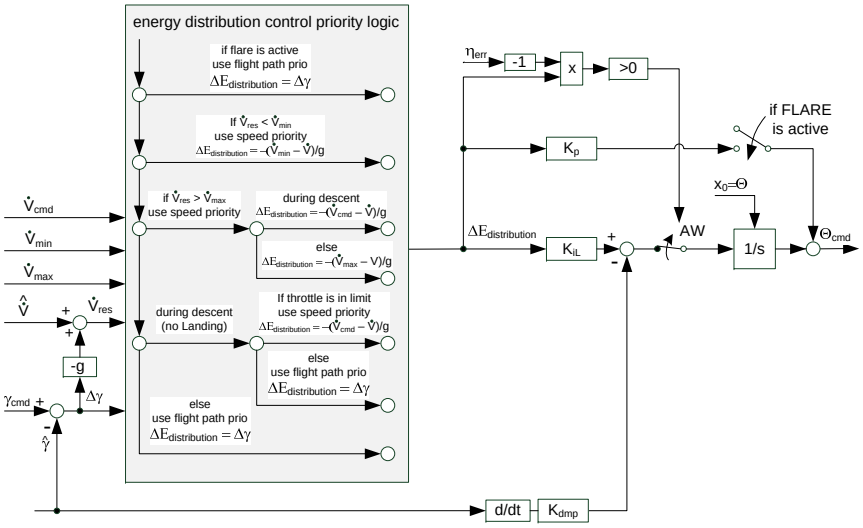

Fig. 9 Scheme of energy distribution control.

A major disadvantage of the used I-controller with additional proportional feedback is the low bandwidth. Therefore, this controller structure cannot be used for flight modes or missions that require a large bandwidth. The low bandwidth is a limit for automatic flare manoeuvres, especially in wind shear, gusty wind conditions or after a steep approach. Lambregts adds in [9] the rate of flight path command $\dot{\gamma}_{cmd}$ as a feed forward signal to the input of the thrust command integrator and to the integral and proportional term of the elevator path. This provides a faster flight path angle response and is used for manual control in *Control Wheel Steering* mode.

In the LAPAZ project, a proportional controller was added to the existing controller structure. It can be activated if necessary. The usage of this proportional component adds a zero to the transfer function and allows to shape and enlarge the bandwidth. So the previous controller structure can be used with this little modification. Niedermeier uses in [13] a similar modification. His energy distribution controller consists of a classical proportional-integral controller (PI-controller). The proportional controller part is always active.

The architecture of the mode logic of the vertical modes is shown in Fig. 10. The structure, introduced in [6] is expanded by the vertical speed limitation and a height protection. By using the vertical speed limitation, the pilot is able to control the direction of energy distribution, as described above. The vertical speed limitation only becomes active if necessary.

The height protection limits flight path commands in order to avoid flights below a minimum height above ground $H_{gnd,min}$. Using the height protection enables safe flight at low heights above ground, which expands the range of possible missions of the utility aircraft. By limiting the commanded flight path angle, instead of a switching, this protection becomes active without transient.

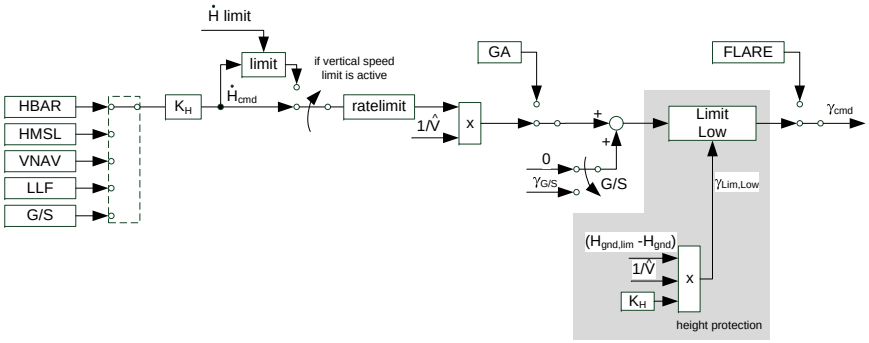

Fig. 10 Mode switching architecture of height and flight path control.

5 Sensor Signals and Filters

The AFCS of the LAPAZ demonstrator has a duo-duplex architecture with redundant sensors, see Fig. 11. The Attitude and Heading Reference Systems (AHRS) are triplex redundant. The Air Data Systems (AD), the Magnetic Sensor Units (MSU) and the height above ground signals from the Laser Altimeters (LA) are duplex redundant. The Global Navigation Satellite System (GNSS) is simplex (no redundancy).

Since simplex sensor signals can only be range checked and cannot be monitored, the integrity of those signals cannot be assured. For safety critical flight control functions and modes, such as flight path control, consolidated sensor signals of high integrity are required. In the S15 demonstrator signals of the flight path angle γ and the ground speed V_{gnd} are only simplex. In an operational system, the redundancy will be duplex or triplex. As the test pilot has to monitor the system behaviour closely to assure flight safety, then simplex sensor signals can be used to demonstrate the Automatic Take-Off and Automatic Landing functions.

The flight path acceleration $\dot{V}_K$ is computed by the body accelerations in longitudinal, lateral and normal direction $n_{x,f}$, $n_{y,f}$ and $\Delta n_{z,f,up}$ and the attitude angles Φ and Θ

$$\dot{V}_K = g \cdot \begin{bmatrix} cos\Theta & sin\Theta sin\Phi & sin\Theta cos\Phi \end{bmatrix} \cdot \begin{bmatrix} n_{x,f} \\ n_{y,f} \\ n_{z,f} \end{bmatrix} \quad . \tag{12}$$

It must be noted, that the body normal acceleration $\Delta n_{z,f,up}$ from the AHRS is zero for stationary horizontal flight. The positive sense is up. It has to be transformed by $n_{z,f} = -(\Delta n_{z,f,up} + 1)$.

The velocity $\hat{V}_A$ is computed, using a complementary filter, see Fig. 12. The true airspeed V_{tas} is passed through a low pass filter with a high time constant ($\tau_1 = 10\,s$) to restrain high-frequency atmospheric turbulence. The resulting lag is compensated by adding the flight path acceleration $\dot{V}_K$. The computed velocity $\hat{V}_A$ is used to com-

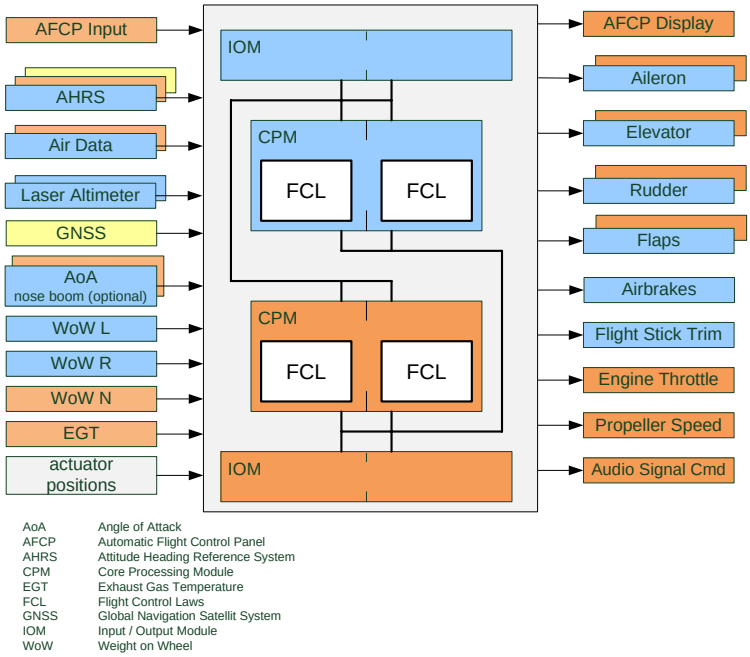

Fig. 11 Architecture of the Automatic Flight Control System.

pute the flight path angle $\hat{\gamma}$ and flight path angle commands from the vertical speed commands.

To take into account wind changes of low bandwidth, e.q. wind shear, low path filtered flight path acceleration $\dot{V}_K$ and airspeed acceleration are added, see Fig. 12. After passing a low pass filter, the complementary filtered acceleration $\hat{\dot{V}}$ is used for total energy control.

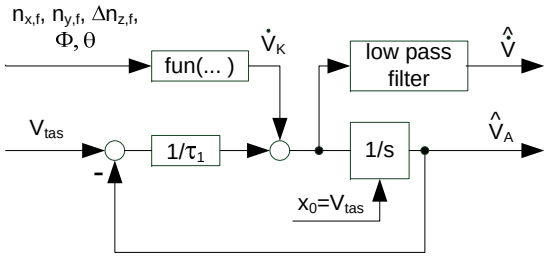

Fig. 12 Block diagram of the velocity and acceleration signal filter.

An observer is used to compute the inertial vertical speed $\hat{\dot{H}}$ from the body normal acceleration $\Delta n_{z,f,up}$ and the barometrical altitude H_{baro}, see Fig. 13. The inertial vertical speed is required to compute the flight path angle.

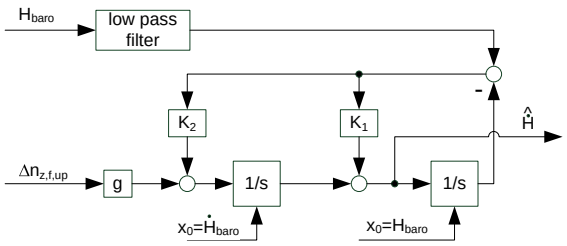

Fig. 13 Block diagram of the vertical speed signal filter.

Beside the flight path angle γ, which can be calculated by the inertial vertical speed and the flight path speed V_K or the ground speed V_{gnd}, an approximated flight path angle $\hat{\gamma}$ is computed by the inertial vertical speed $\dot{H}$ and the complementary filtered velocity $\hat{V}_A$

$$sin(\hat{\gamma}) = \frac{\hat{\dot{H}}}{\hat{V}_A} \quad . \tag{13}$$

The flight path angle γ is used for earth referenced missions, like glide slope tracking. The estimated flight path angle $\hat{\gamma}$ is used for airmass referenced missions, e.g. altitude changes with given vertical speeds. By using this signal, vertical speed following in wind conditions can be achieved, since the energy, induced by wind to the system, can be considered.

If there is no wind, flight path angle and estimated flight path angle are the same ($\gamma = \hat{\gamma}$). In Fig. 14, the geometric interrelation of the wind, the flight path angle and the computed flight path angle is shown in the longitudinal vertical plane. With increasing wind, the difference between both angles increases.

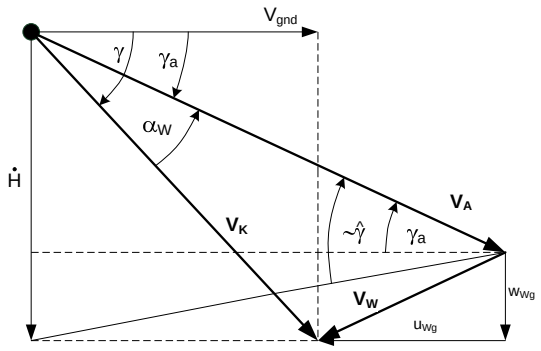

Fig. 14 Geometric interrelation of the wind, the flight path angle and the computed flight path angle.

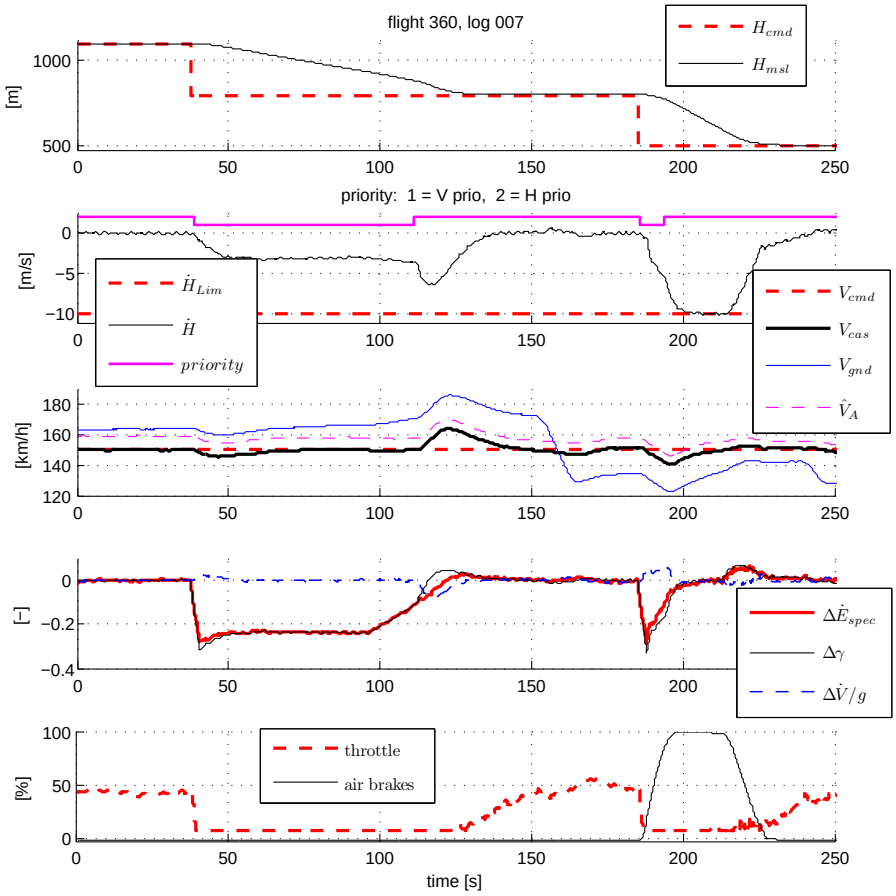

Fig. 15 Flight test results, comparison of sink performance with and without use of airbrakes.

6 Flight Tests Results

The first automatic flight took place in August 2010. Since then, more than 80 hours of successful flight tests were done with the AFCS. In these test flights the TECS function was validated. The first successful automatic landing took place on March 22nd, 2012.

The performance of TECS with and without airbrakes was investigated in flight. Figure 15 shows a time plot of two descents, commanded by steps in height of $\Delta H_{cmd} = -300\,m$. The vertical speed limit was set to $\dot{H}_{Lim} = -10\,m/s$. The target is to reach $\dot{H}_{Lim}$ during the descent. The commanded airspeed of $V_{cas} = 150\,km/h$ should be kept constant. The use of the airbrakes for total energy control was optionally activatable.

Between t=0 s and 150 s the airbrakes were not used. After t=150 s the airbrakes were used. In the first descent without airbrakes, the throttle was commanded to idle position. The maximum speed protection was detected and the speed priority was activated. The elevator controls the commanded velocity, see the *energy distribution control priority logic module* in Fig. 9. The small airspeed deviation at the beginning of the descent, that was induced by the fast reduction of the thrust, was quickly reduced. The sink rate approached a constant value of $\dot{H} \approx -3\,m/s$. The vertical speed command of $\dot{H}_{Lim} = -10\,m/s$ was not reached. Shortly before reaching the commanded height, the FCL switched from speed priority to flight path priority. This caused direct reaction of the airspeed which increases by 14 km/h and the vertical speed which increases by 2.5 m/s. This behaviour is not satisfactory. Here some work has to be done. The throttle was commanded in time to maintain the airspeed and the height. At t=150 s the aircraft makes a 90° left turn into the wind, which can be seen at the ground speed, which reduces from approximately 170 km/h to 135 km/h. During the turn, the height and the calibrated airspeed were maintained very well.

In the second descent, starting at t≈180 s, the use of the airbrakes was allowed. After the new height command, the FCL commanded the throttle to idle and extended the airbrakes to improve the sink rate. After switching to speed priority due to a detection of maximum speed protection, the flight continues with flight path priority, since the calculated value $\dot{V}_{cmd,res} = -\Delta\gamma \cdot g + \dot{V}$ falls below $\dot{V}_{max}$ due to reduction of $\Delta\gamma$. The vertical speed command of $\dot{H}_{Lim} = -10\,m/s$ was reached and well maintained without overshoot, the deviation between the commanded flight path and the flight path $\Delta\gamma$ goes to zero. The initial velocity error of 9 km/h is caused by the rapid reduction of the thrust and by the subsequent airbrake extension. After that the deviation in the velocity is slowly reduced. Shortly before reaching the commanded height, the airbrakes are retracted and the throttle is commanded in time. Since the sink rate was larger in the second descent than in the first, the descent time was shorter. As the descent took place with maximum airbrake deflection and with the throttle at its minimum limit, it demonstrates the maximum sink performance of the airplane for this configuration and this airspeed.

In another flight test, a descent was commanded ($\Delta H_{cmd} = -1000\,m$) with varying commands of vertical speed, see Fig. 16. The first vertical speed command was $\dot{H}_{Lim} = -10\,m/s$. This was reduced to $\dot{H}_{Lim} = -8\,m/s$ and after that to $\dot{H}_{Lim} = -6\,m/s$. The function which uses the airbrakes as control element was active. Directly after the descent command, the throttle was commanded to idle. The descent begins with speed priority and continues with path priority, like in the flight test described before. The controlled aircraft follows the given vertical speed commands well. The airbrakes were commanded as needed. The error in the total energy rate was reduced rapidly. The error in velocity reduces slowly, while the tailwind reduces, which shows a comparison of the ground speed V_{gnd} and the calibrated airpseed V_{cas}.

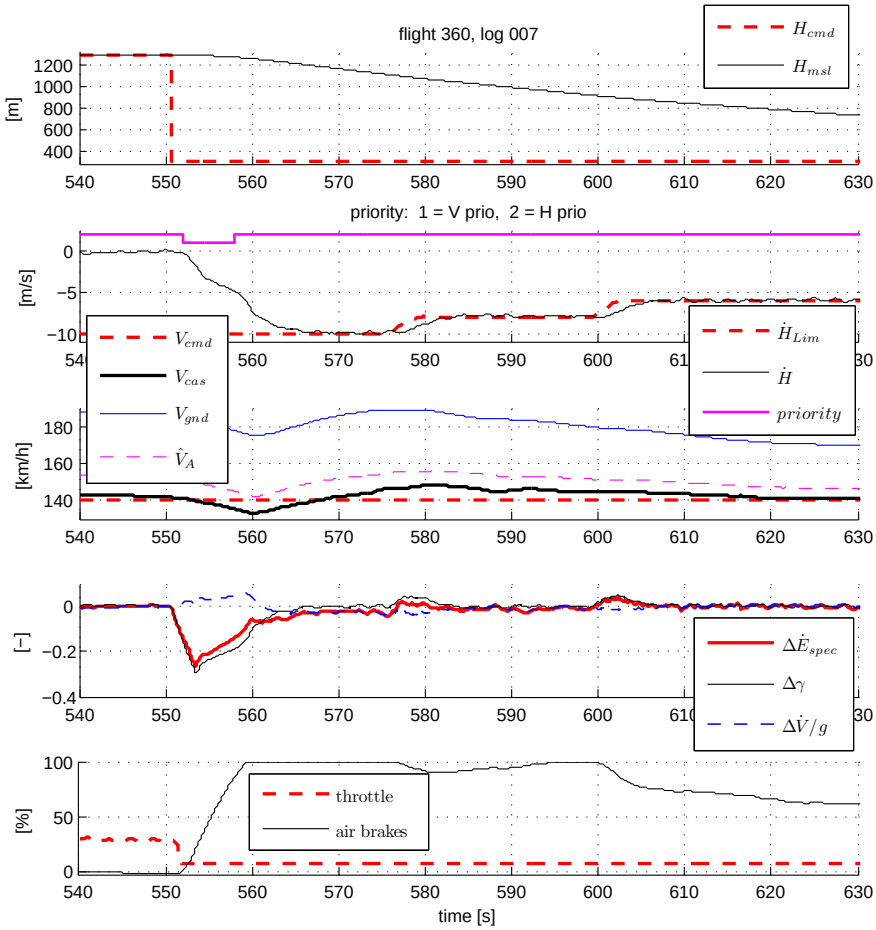

Fig. 16 Flight test results, variation of presettings for vertical speed.

7 Conclusion

The TECS concept, introduced by Lambregts, was taken up, modified and extended and tested in flight. The additional use of airbrakes proved to be an adequate possibility to manipulate the total energy of a aircraft and to extend the sink performance. This allows flying steeper vertical flight path missions. The function was validated in flight with satisfactory results. Improvements of speed and flight path accuracy during transient behaviour, i.e. transition from descent to horizontal flight without using airbrakes are under investigation.

References

1. Bruce, K.R.: NASA B737 Flight Test Results of the Total Energy Control System, AIAA Guidance, Navigation and Control Conference, AIAA 86-2143 CP, August 1986
2. Bruce, K.R.: NASA B737 Flight Test Results of the Total Energy Control System, NASA Contractor Report 178285, January 1987
3. Bruce, K.R.: Integrated Autopilot/Autothrottle Based on a Total Energy Control Concept: Design and Evaluation of Additional Autopilot Modes, NASA Contractor Report 4131, APRIL 1988
4. Bruce, K.R.: Integrated Autopilot/Autothrottle for the NASA TSRV B-737 Aircraft: Design and Verification by Nonlinear Simulation, NASA Contractor Report 4217, 1989
5. Dalldorff, L., Luckner R., Reichel R.: A Full-Authority Automatic Flight Control System for the Civil Airborne Utility Platform S15 – LAPAZ, Euro GNC 2013
6. Lambregts, A.A.: Vertical Flight Path and Speed Control Autopilot Using Using Total Energy Principles, AIAA Paper 83-2239, August 1983
7. Lambregts, A.A.: Integrated System Design for Flight and Propulsion Control Using Total Energy Principles, AIAA Paper 83-2561, October 1983
8. Lambregts, A.A.: Functional Integration of Vertical Flight Path and Speed Control using Energy Principles, 1st Annual NASA Aircraft Controls Workshop, October 25-27, 1983, NASA LRC.
9. Lambregts, A.A.: Total Energy Based Flight Control System, World Intellectual Property Organization, International Publication No. WO 84/01345, April 12, 1984
10. Lambregts, A.A.: Total Energy Based Flight Control System, United States Patent No. 6,062,513, May 16, 2000
11. Lamp, M.: Flight Control Law Development for the Automatic Flight Control System LAPAZ, Euro GNC 2011, April 2011
12. Looye, G.H.N.: An Integrated Approach to Aircraft Modelling and Flight Contorl Law Design, PhD Thesis, 2007, ISBN/EAN: 978-90-5335-148-2
13. Niedermeier, D., Lambregts, A.A.: Design of an intuitive Flight Control System, CAES 2009
14. Subhabrata Ganguli, Balas G.: A TECS Alternative using Robust Multivariable Control, AIAA 2001-4022
15. U.S. Department of Transportation, Federal Aviation Administration, Air Traffic Organization Operations Planning, Office of Aviation Research and Development, Washington, DC 20591. : Advanced Guidance and Control - Operational and Safety Benefits, Report No. DOT/FAA/AR-08/27, June 2008